Published in
Deformation Mechanisms, Rheology and Tectonics : from Minerals to the Lithosphere 243 : 295-310, 2005,
which should be used for any reference to this work

Origin of the current stress field in the western/central Alps: role of gravitational re-equilibration constrained by numerical modelling

BASTIEN DELACOU, CHRISTIAN SUE, JEAN-DANIEL CHAMPAGNAC & MARTIN BURKHARD

Institut de Géologie, Université de Neuchâtel, Switzerland

Abstract: We interpret the strain and stress fields of the western/central Alpine arc on the basis of 2.5D finite element modelling and a recent seismotectonic synthesis. Models have fixed boundary forces and different crustal geometries, so that they respond to buoyancy forces (variations in gravitational potential energies). The seismotectonic regime, characterized by orogen-perpendicular extension in the high topographic core of the belt and local orogen-perpendicular compressional/transpressional deformation in the external zones, appears to be very close to the modelled gravitational regime. Rotation of Apulia has a minor effect on the current strain or stress fields of the Alpine realm. Nevertheless, it could help to explain the orogen-parallel dextral faulting that is observed all along external zones, from the northern Valais to the Argentera external crystalline massif. Our results highlight the consequences for the Alpine realm of ongoing convergence between the African and European plates. Our interpretation is that collision is no longer ongoing and that buoyancy-driven stresses dominate the present-day geodynamics of the western/central Alps.

The Alpine belt has resulted from Tertiary collision between the Apulian micro-plate (considered as an African promontory) and the European plate, following Late Cretaceous to Eocene subduction of the Alpine Tethys (Coward & Dietrich 1989; Dewey *et al.* 1989; Laubscher 1991; Stampfli *et al.* 1998; Schmid & Kissling 2000). Whereas compressional structures, such as nappes, metamorphic zones and phases of folding have been well documented (e.g. Choukroune *et al.* 1986; Fry 1989; Burkhard 1990; Pognante 1991; Butler 1992; Spalla *et al.* 1996; Duchêne *et al.* 1997; Burkhard & Sommaruga 1998; Becker 2000) the current tectonic context remains debatable. Is collision still active or has the Alpine belt come to the end of its compressive history? The relatively recent discovery of extensional tectonics, through seismotectonic and structural analyses (Mancktelow 1992; Maurer *et al.* 1997; Eva *et al.* 1998; Fügenschuh *et al.* 1999; Sue *et al.* 1999; Bistacchi *et al.* 2000; Kastrup 2002; Sue & Tricart 2002, 2003; Champagnac *et al.* 2003; Champagnac *et al.* 2004) goes a long way toward answering the question. Extensional earthquakes have been known for a long time (Pavoni 1961; Ahorner *et al.* 1972; Fréchet 1978). The large-scale seismotectonic synthesis of Delacou *et al.* (2004) demonstrates that an extensional regime operates throughout all the internal zones of the belt. In addition, structural analyses of fault slip data indicate that extensional tectonics have been prevalent in these zones since at least Miocene times (Mancktelow 1992; Bistacchi *et al.* 2000; Tricart *et al.* 2001; Sue & Tricart 2003; Champagnac *et al.* in press). Extension is therefore a major feature of the recent to present-day geodynamics of the Alpine arc. Various contradictory models have been put forward to explain such intra-orogenic extensional tectonics: (1) large-scale buckling under compressive conditions combined with outer-arc extension (Burg *et al.* 2002), (2) lateral extrusion in an active convergent belt (Ratschbacher *et al.* 1991; Frisch *et al.* 2000; Sachsenhofer *et al.* 2000), (3) slab break-off re-equilibration (Davies & von Blanckenburg 1995; Sue 1998), (4) rotational tectonics (Calais *et al.* 2002; Collombet *et al.* 2002), and (5) gravitational re-equilibration of an over-thickened crust (Bada *et al.* 2001). While overall convergence between the African and European plates is still ongoing at a rate of 3 to 8 mm a^{-1} (Argus *et al.* 1989; Demets *et al.* 1994; Albarello *et al.* 1995; Crétaux *et al.* 1998; Nocquet 2002), the boundary conditions

around the Alpine belt, as estimated by recent GPS results (Calais *et al.* 2002; Nocquet 2002; Vigny *et al.* 2002; Nocquet & Calais 2003, 2004), reveal no clear relative movements between the Apulian and European microplates. Velocities across the belt are between 1 and 2 mm a^{-1} and they provide no clear indication of convergence or divergence. At best, the GPS data indicate anticlockwise rotation of Apulia with respect to Europe at an angular velocity of 0.52°/Ma, about a pole near Milan (Calais *et al.* 2002).

In this study we use numerical modelling and the large-scale seismotectonic analysis of Delacou *et al.* (2004), to test the effects of gravitational body forces, coupled with rotation, on the current stress and strain fields of the western/central Alps. Numerical modelling has proved to be a powerful tool for analysing the geodynamics of different areas, such as the Himalayas (Cattin & Avouac 2000; Cattin *et al.* 2001), New Zealand (Liu & Bird 2002), southern Spain and northern Africa (Negredo *et al.* 2002), the United States and Mexico (Bird 2002), the Baikal rift zone (Lesne *et al.* 1998), the Basin and Range province (Hassani & Chéry 1996) and Central Europe (Grünthal & Stromeyer 1992; Golke & Coblentz 1996). Here, we use a three-dimensional model of the Alps to study the origins of the current stress and strain fields of the western/central Alpine arc.

Seismotectonic data

We test our numerical models by comparing calculated strain and stress fields with those obtained from earthquake analysis (Delacou *et al.* 2004). Our database is a compilation of 389 reliable focal mechanisms (Ménard 1988; Thouvenot 1996; Eva & Solarino 1998; Sue *et al.* 1999; Baroux *et al.* 2001; Kastrup, 2002), covering the entire arc of the western/central Alps, from eastern Switzerland to the Ligurian margin (Fig. 1). Local magnitudes (Ml) range from 0.7 to 6.0, for earthquakes recorded between 1969 and 2000. Foci are mainly in the upper crust (first 20 km), especially in the core of the belt where no deeper earthquakes have occurred. There are a few exceptions in external areas (30 km under the Swiss Molasse basin, 25 km under the western Po plain and 20 km under the Ligurian margin).

Seismotectonic strain and stress fields

The strain and stress states of the Alpine realm are defined via three parameters (Fig. 1): type of deformation (compressional, extensional or transcurrent), principal directions of deformation (P- and T- axes) and principal stress axes ($\sigma 1$, $\sigma 2$, $\sigma 3$) obtained from inversion of focal plane solutions.

We used the dips of P- and T-axes to calculate an r-parameter (P-axis dip − T-axis dip) that summarizes the type of deformation, that is, compressional, extensional or transcurrent (Delacou *et al.* 2004). In Figure 1 the r-parameter is shown by coloured dots at epicentres, whereas interpolation provides the background colour. This large-scale regionalization reveals large zones of homogeneous deformation. In the internal zones, a continuous zone of extension follows the crest line from the southern Valais to the Argentera massif. Extension is also found in eastern Switzerland, over topographic highs, but continuity with the main zone is not proven, because the Lepontine dome is almost seismically active. Other notable features are local zones of compressional/transpressional deformation along the edges of the Alpine belt, in the eastern Helvetic domain, the front of the Belledonne massif, the front of the Digne nappe and the western Po plain.

We made a map of P- and T-axis trajectories, by projecting the axes onto a horizontal plane and interpolating vectorially (Fig. 1). In internal zones, orogen-perpendicular extension prevails, T-axes striking N–S in the Valais, E–W behind the Pelvoux massif, and SW–NE behind the Argentera massif. In external zones, P-axis trajectories define a large-scale fan, convergent toward the Po plain. Orogen-perpendicular compressive axes swing through 120°, from a NNW trend in eastern Switzerland, to NW in front of the Belledonne massif, and SW in front of the Digne nappe. This orogen-perpendicular configuration confirms earlier results, which were based on far fewer data (Fréchet 1978; Pavoni 1986).

Stress inversion methods have been applied to subsets of the focal mechanism data, to constrain the present-day stress field of the Alpine arc. For details of the analysis and calculations, see Delacou *et al.* (2004). The results (Fig. 1) reveal a generalized extensional stress field in the core of the belt. Orogen-perpendicular $\sigma 3$, contrasts with localized zones of transpression in external zones, where fan-shaped orogen-perpendicular $\sigma 1$ converges toward the Po plain. Strike–slip faulting occurs everywhere in the belt, but is especially abundant in external zones.

Correlations with crustal thickness

We have used a Digital Elevation Model (DEM), GTOPO30, to calculate average Alpine

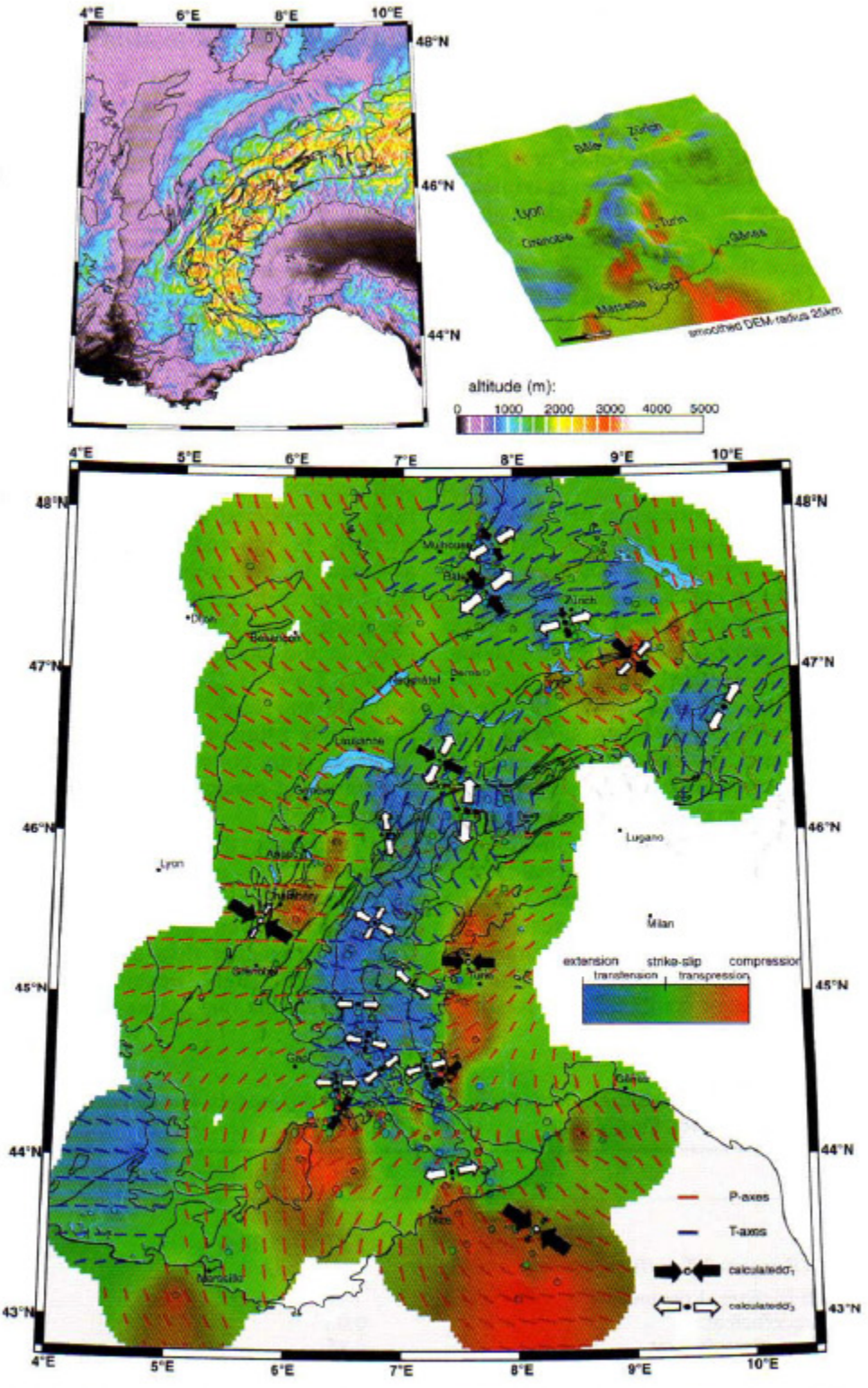

Fig. 1. Seismotectonic overview of the study area (Delacou *et al.* 2004). *Top.* Left: Digital elevation model (DEM) and geological contours. Note correspondence between topographically high areas and extensional zones of deformation (bottom map). Right: Regionalization of deformation draped on smooth DEM (radius 25 km). Note extension in inner areas that follows crest of belt and localized compressive/transpressive areas at feet of topographic gradients. *Bottom.* Strain and stress fields of the Alpine realm. Background colour represents type of deformation, small coloured lines represent earthquake P-axes (red) and T-axes (blue), black arrows are $\sigma 1$ axes and white arrows $\sigma 3$ axes. Note the orogen-perpendicular pattern of both tensile axes (in the core of the belt) and compressive axes (in external areas).

topography, where each point of the grid represents average altitude within a radius of 25 km (Fig. 1). This average topography provides a proxy for topographic loading at the scale of the lithosphere, high average altitude being associated with over-thickened crust. The resulting map closely matches gravimetric maps (e.g. Masson *et al.* 1999), high average topography (higher than 2500 m) corresponding to strong negative Bouguer anomalies (−160 to −220 mgal). On draping the map of regionalized deformation over the average DEM (Fig. 1), internal areas of high topography appear to match closely with areas where the state of strain/stress is extensional. In contrast, transpressive external zones coincide with zones of concave-upward curvature, between high mountains and low foreland.

To explain the close correlation between areas of large crustal thickness (directly correlated with high average topography) and generalized Alpine extensional tectonics, we favour a geodynamic model, where the current Alpine regime is controlled, at least partly, by internal gravitational body forces. In this model, gravitational potential anomalies (GPA), driven by crustal thickness heterogeneities between internal and external zones, will induce extension in high internal zones. In response to this extensional regime, external areas will undergo compression/transpression. This kind of model will induce orogen-perpendicular extensional stress axes in high internal zones and orogen-perpendicular compressional stress axes in low external zones. In what follows, we use numerical techniques to test this model of gravitational re-equilibration, alone or combined with rotation.

2.5D finite element modelling

A numerical code (2.5D thin-shell finite element code, SHELLS) has been used to model the stress and strain field of the western/central Alpine arc. Basically, this code solves for stress equilibrium and conservation of mass, given the rheology and density at each point (Bird 1989, 1999; Kong & Bird 1995). Models include three-dimensional variations in topography and thickness of crust and lithosphere. Because the code solves a momentum equation in a vertically integrated form (two-dimensional approximation), it is referred to as a 2.5D finite element method. The thin-shell approximation yields only horizontal components of the momentum equation (the vertical component being replaced by an isostatic approximation) and no vertical shear traction is considered on vertical planes (flexural strength is ignored). Material behaviour is assumed to be anelastic: thermally activated non-linear dislocation creep in the lower crust and mantle, and Mohr–Coulomb frictional plasticity in the shallow parts of crust and upper mantle (Table 1). Given values of initial surface heat flow and steady thermal conduction are used to compute a three-dimensional temperature distribution with constant but distinct heat productivity and conductivity for crust and mantle (Table 1).

In summary, the assumptions and approximations of this method enable modelling of large-scale geodynamic systems over long time-scales (given the anelastic assumption, time-scales smaller than a few thousand years are not adequately modelled). For orogenic systems like the one in this study, the thin-shell

Table 1. *Thermal parameters, densities and rheological parameters of models. For detailed description of rheological parameters, see Bird (1989)*

Parameter	Values (crust/mantle)	Units
Heat conductivity	2.7/3.2	$J\,m^{-1}\,s^{-1}\,K^{-1}$
Heat productivity	7.27E-7/3.2E-8	$J\,m^{-3}\,s^{-1}$
Mean densities ($P = 0$ and $T = 0$)	2816/3332	$kg\,m^{-3}$
Mohr–Coulomb frictionnal parameters		
Fault friction coefficient	0,03	
Continuum friction coefficient	0,85	
Biot coefficient (efficacy of pore pressure)	1	
Dislocation-creep parameters		
ACREEP (shear stress coefficient)	2.3E9/9.5E4	$Pa\,s^{1/3}$
BCREEP (temperature coefficient)	4000/18 314	K
CCREEP/G/p (pressure coefficient)	0/0.0171	$K\,Pa^{-1}$
DCREEP (max. shear stress)	5.00E + 08	Pa
ECREEP (exponent) $= 1/n$	0.333333	

code can efficiently model the response to gravitational potential anomalies (GPA), but will not account for flexural strength (or isostatic rebound). However, even in processes such as post-glacial rebound or erosional denudation, where flexure is a significant component, the models would probably yield a stress pattern that is close to the one indicated by earthquakes (that is, extensional tectonics in internal uplifted areas). Another limitation of the 2.5D approximation is that decoupling of the stress field cannot occur at depth. Thus, it is not possible to model compression in the deep lithosphere and simultaneous extension at shallower depths. However, this limitation may not be serious, because no vertically decoupled tectonics of this kind have yet been identified at a large scale in the Alpine arc.

Given the assumptions, the models in this study are limited to the analysis of the stress or strain field generated by re-equilibration of gravitational potential anomalies (GPA) and its possible combination with rotational tectonics.

The boundaries of the models have been chosen to reflect the limits of the western/central Alps, as well as the limits of our seismotectonic study (Fig. 2). In the north, the boundary follows the outer edge of the Molasse Basin; in the northwest and west, the outer edges of the Jura and Subalpine chains; in the southwest, the lower Rhone valley; in the south, the Ligurian margin; and in the southeast, the Po plain. The eastern boundary of the model is an arbitrary north–south line, which is assumed to be frictionless and that limits our study area to the western/central Alps. The models in this study all have 295 cells, used in the finite element technique (Fig. 2).

Another feature of the code SHELLS is that it can take into account faults (Fig. 2, Table 1). In the western/central Alps, the problem has been to identify large faults that are potentially active. Indeed, recognized seismically active faults are scarce and of limited extents. Moreover, an exhaustive list of active faults is difficult to establish, as every new local seismic swarm defines a new active fault system. In our models, we have decided to take into account large-scale inherited structures that are supposed to play an important role in the current dynamics of the studied area, these being the Pennine front and the Insubric line (Fig. 2).

Models with fixed boundaries

In order to test the effects of buoyancy forces alone, models are assumed to have fixed boundaries. The strain/stress field is generated only by contrasting gravitational potential anomalies (GPA) between the inner areas of thickened crust and external normal ones.

Isostatic model (model A)

As a first step, a simple three-dimensional model has been constructed under the assumption of isostatic equilibrium (Figs 3 and 4). From the surface topography (taken from the GTOPO30 DEM data, smoothed at the mesh spacing size) and the surface heat flow (compiled from the European Geotraverse experiments; Blundell *et al.* 1992), SHELLS calculates routinely the three-dimensional structure of the crust and the lithosphere that satisfies isostatic equilibrium (Fig. 3) and steady-state thermal conduction, by taking into account the densities and thermal properties of crust and mantle (Table 1). We assume that all boundary nodes are stationary.

For model A, the calculated stress field is characterized by orogen-perpendicular extension in regions of high topography in the core of the belt and by orogen-perpendicular compression in external zones (Fig. 4). This pattern results from equilibration between regions of positive GPA in the inner areas, where high topography correlates with large crustal thickness (according to the assumption of isostatic equilibrium) and regions of normal GPA (near zero) in external zones, where altitudes are small and the Moho is close to its normal depth (around 30 km). This configuration results in an extensional stress state in the core of the belt, tending to reduce the over-thickened crust, and a compressional stress state in external regions.

In terms of strain rate (Fig. 4), a belt of horizontal stretching appears to follow the high topography, especially on its external side, from the Aar massif to the Argentera massif. Extensional strain rates are between 1 and 7×10^{-16} s^{-1}. Compressional strain rates are about 2×10^{-16} s^{-1} in external zones. They seem to be guided by the fixed boundaries of the model, reaching a maximum in front of the Jura, the Po plain and the Rhone valley. This could be explained by GPA equilibration, whereby crustal thickness decreases over the whole system as far as the boundaries of the model, where it creates compression. In reality, external boundaries (that can be considered as fixed, far away from the Alps) are not as sharp as they are in our models, so that shortening should be more distributed.

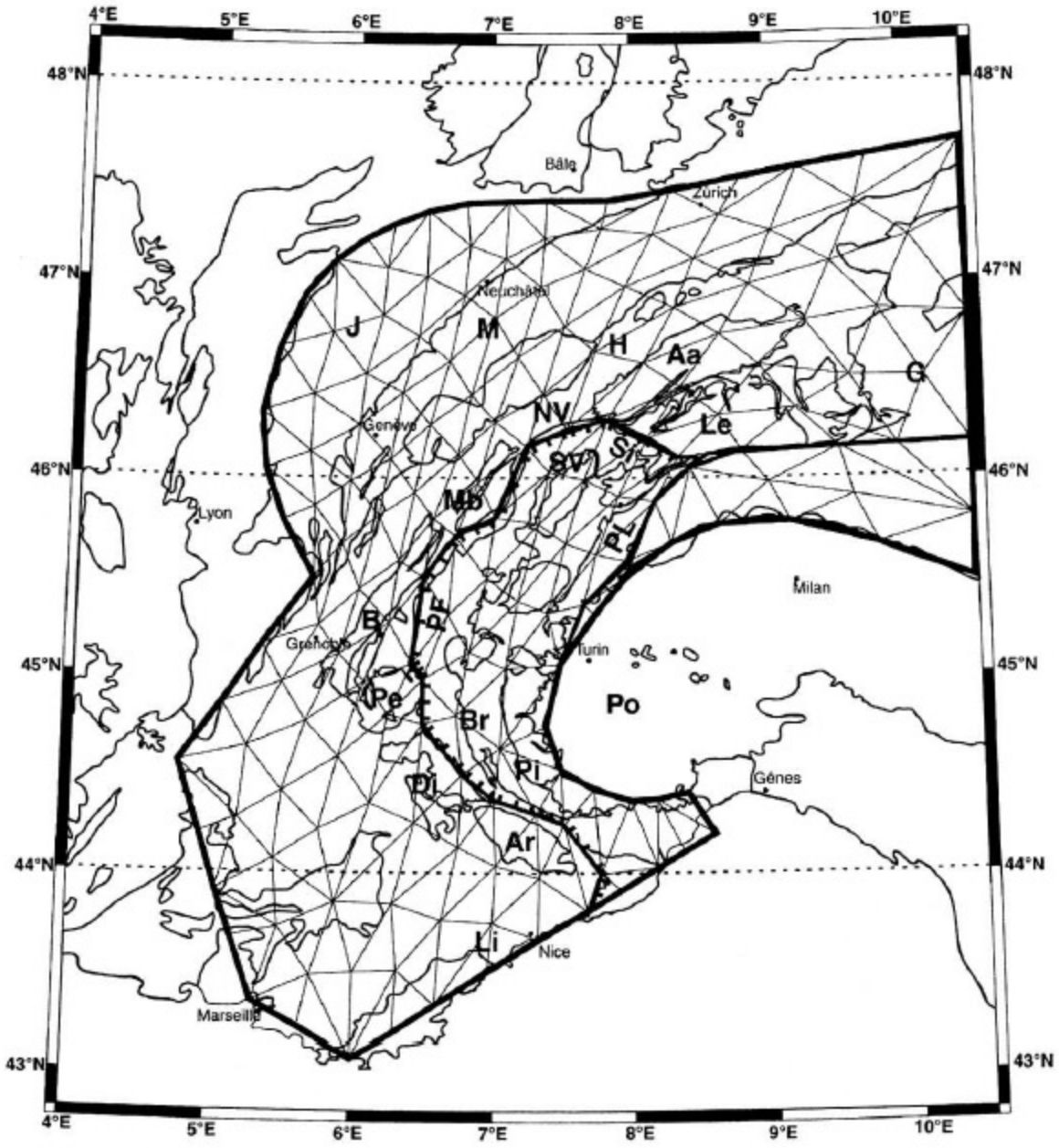

Fig. 2. Grid and configuration in our finite element models. Models have 295 elements, regularly spaced in the area of the western/central Alps. Bold lines inside models represent faults: Pennine Front (PF), Simplon fault (Si) and Periadriatic Line (PL). Aa, Aar external crystalline massif; Ar, Argentera external crystalline massif; B, Belledonne external crystalline massif; Br, Briançonnais area; Di, Digne nappe; G, Grisons; H, Helvetic zones; J, Jura fold and thrust belt; Le, Lepontine dome; Li, Ligurian margin; M, Molasse basin; Mb, Mont-Blanc external crystalline massif; NV, Northern Valais; Pi, Piemontais area; Pe, Pelvoux external crystalline massif; Po, Po plain; SV, Southern Valais.

The surface velocity field also follows the shape of the model, velocities reaching about 0.15 to 0.25 mm a^{-1} in directions (NW to SW) that are perpendicular to the belt. In internal zones, stretching leads to southeast-directed surface velocities, which reach 0.3 mm a^{-1} in the northern part (Valais).

Motion on faults is mainly manifest as extensional reactivation of the Pennine front. Slip perpendicular to this fault zone reaches 0.7 mm a^{-1} on its northern segment and decreases progressively toward the south. Near the Mediterranean, the fault appears to be locked. The Periadriatic line does not slip at all.

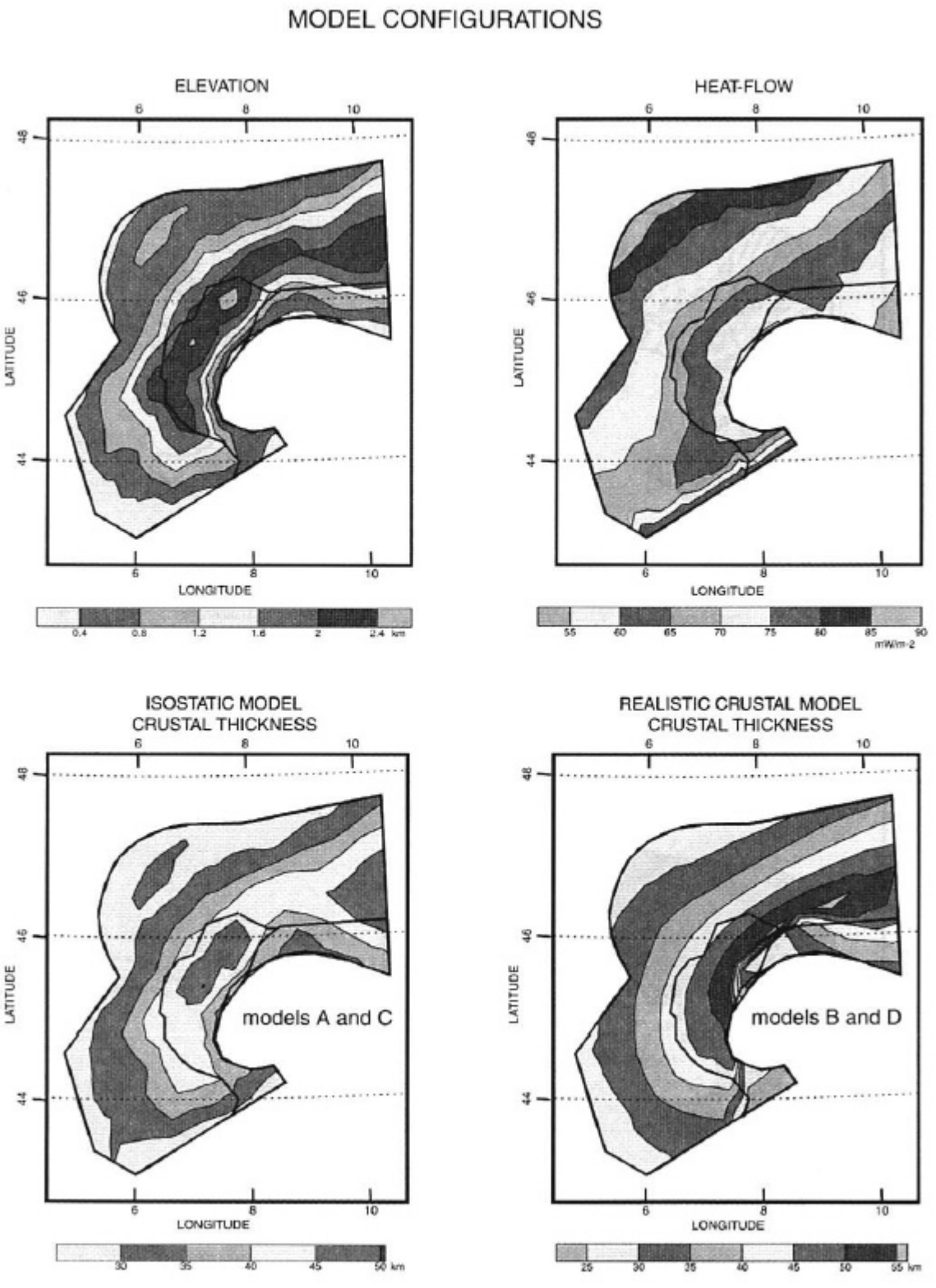

Fig. 3. Model configuration. Elevation and surface heat flow are common to all models. Note differences in crustal thicknesses between isostatic models (models A and C), where Moho depth is directly related to topography, and realistic models (models B and D), characterized by a Moho dipping toward the E/SE on the European side of the belt, and a complex geometry at the eastern Po plain boundary. Moho geometry is taken from Waldhauser *et al.* (1998).

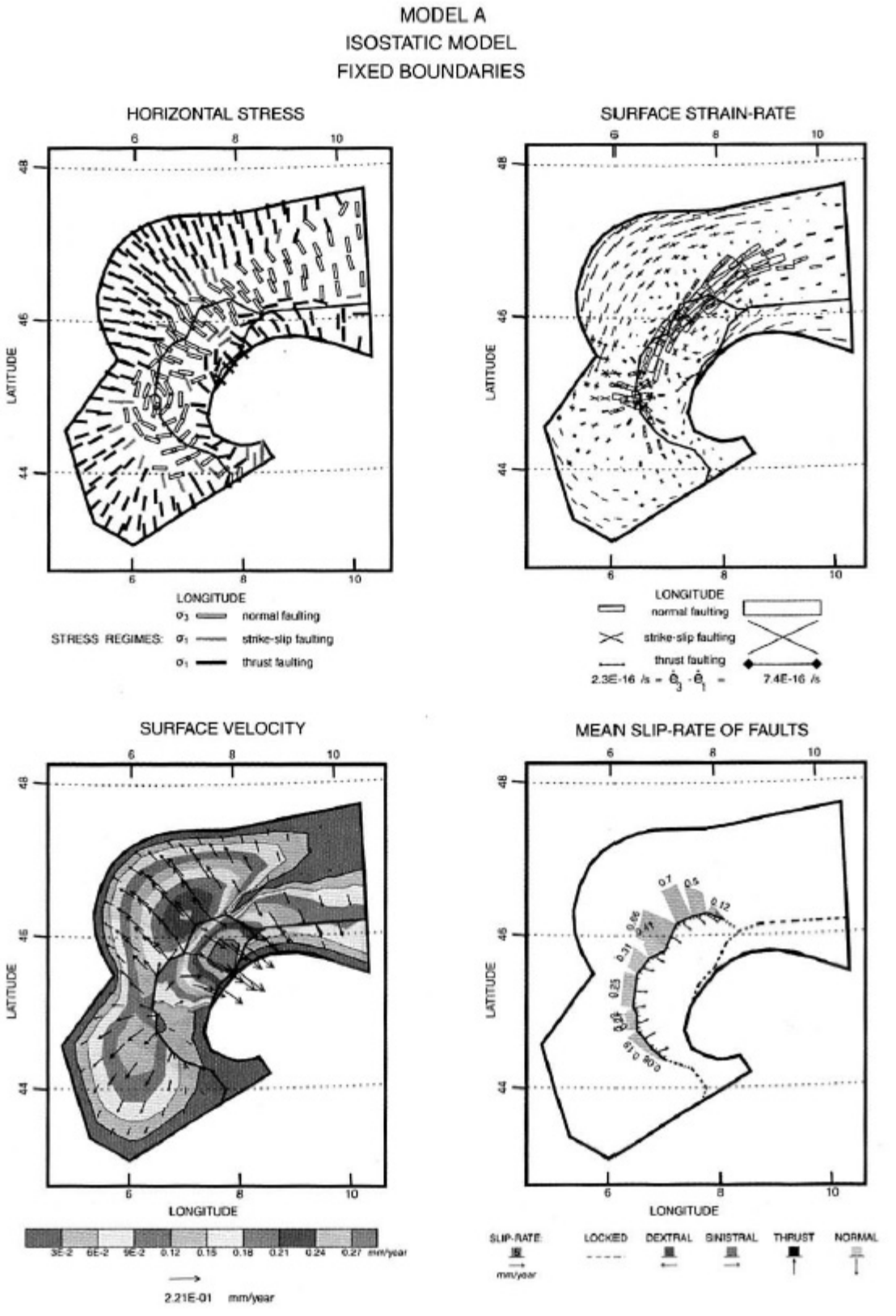

Fig. 4. Model A: Model with isostatic three-dimensional crustal geometry (see Fig. 3) and fixed boundaries. This starting model represents tectonic response of Gravitational Potential Anomalies (GPA) in a simple model of the western/central Alps (see text for explanations).

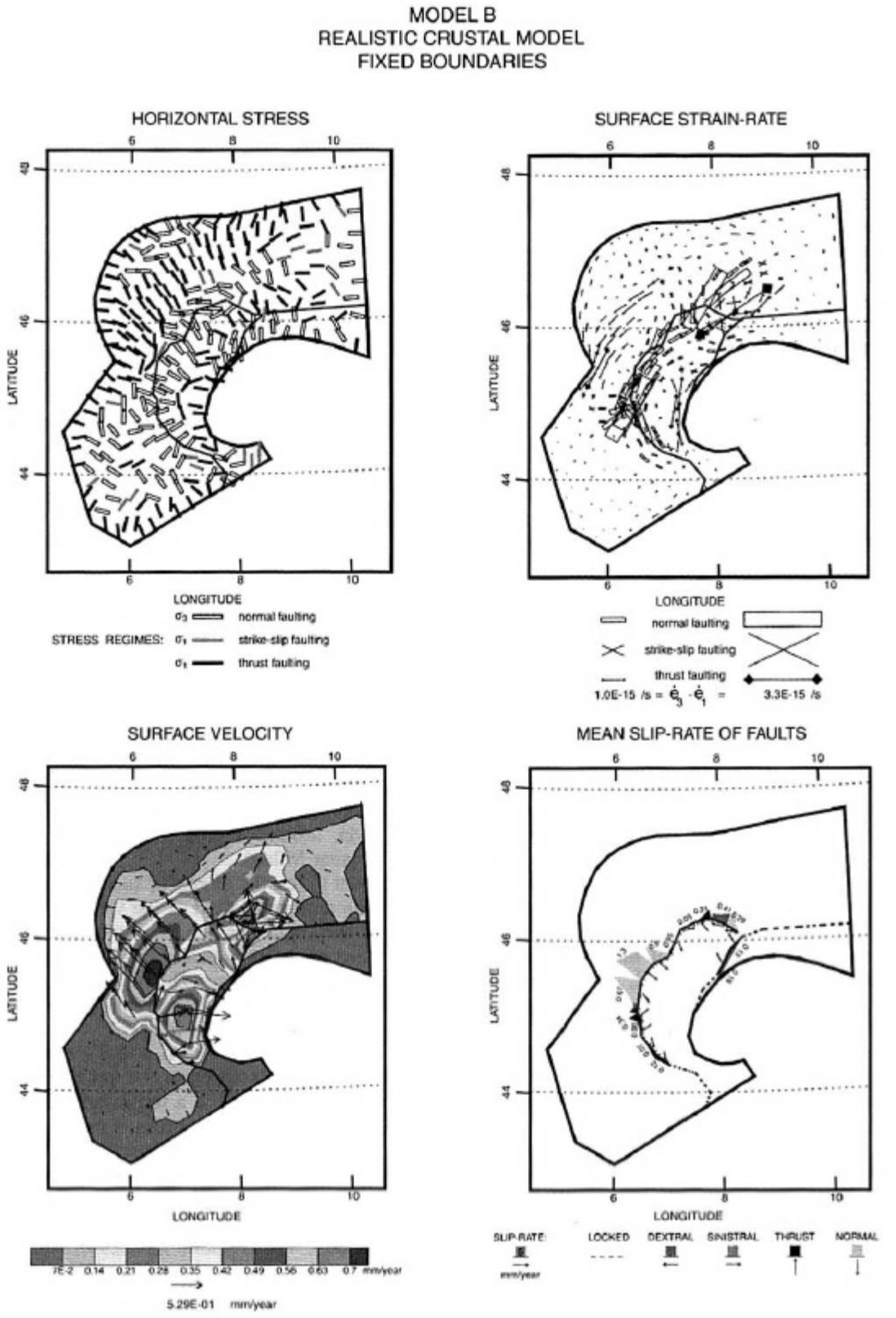

Fig. 5. Model B: Model with realistic three-dimensional crustal geometry (see Fig. 3) and fixed boundaries. This model exhibits a more complex tectonic response than model A, as a result of complex crustal geometry (see text for explanation).

Realistic crustal model (model B)

For a more realistic three-dimensional crustal structure, we have constructed a model (model B, Fig. 5), where the Moho geometry (Fig. 3) has been interpreted from wide-angle seismic experiments (Waldhauser *et al.* 1998). Given the topography, surface heat flow and realistic crustal geometry, lithosphere thickness is calculated, so as to respect the thermal properties of crust and mantle (assuming steady thermal conduction). This results in a complex three-dimensional geometry (Fig. 3), where the highest altitudes do not directly overlie the crustal root. The latter reaches a depth of about 50–55 km at a point that appears to be shifted toward the SSE with respect to large-scale topography. A consequence of such a setting is that GPAs do not correlate in a simple manner with topography (as they do in model A), but depend on the whole three-dimensional crustal structure. In regions of high topography and relatively shallow Moho depth, the GPA is positive and extension is expected in the anomalous lithosphere, whereas in regions of deep Moho and relatively moderate topography, the GPA is negative and compression is expected. Thus, the resulting stress field (Fig. 5), appears to be more complex than in model A. A general trend, from inner extension to outer compression, is still present (as in model A), but with regional variations. This is so in the Jura, where extension now occurs in the northern inner part, in the southwestern external Alps, where there is a mix of compression and extension, and in the northwestern Po plain, where extension is observed. These can be considered as local effects of crustal thickness variations, which were not present in model A. In the southwestern Alps, where focal mechanisms are of mixed type (compressional, extensional and transcurent), the model seems to fit the observations. In the northern part of the internal zone, the general orogen-perpendicular extension is cross-cut by an E–W band of N–S extension. This correlates with the northern edge of the Apulian crustal wedge (Fig. 3), which may be correlated to the Val d'Aosta extensional fault zone (Bistacchi *et al.* 2001). Three bands of high strain rate (up to 3×10^{-15} s^{-1}) can be recognized: a band of WNW–ESE shortening in the external zones beyond the Belledonne and Mont-Blanc massifs, a band of fan-shaped stretching that follows the topographic high (with two peaks in the Aar and Pelvoux regions), and E–W shortening in the western Po plain. These bands correlate fairly well with the seismotectonic setting and the concentrations of epicentres (see Fig. 1). There are three zones of high surface velocities: NW-directed velocities of up to 0.75 mm a^{-1} in external zones, E-directed velocities of up to 0.7 mm a^{-1} in the southern inner area, and a complex zone over the Aar massif.

The pattern of slip along faults is more complex than in model A. Extensional fault slip (up to 1.3 mm a^{-1}) occurs along the middle segment of the Pennine front, whereas the northern branch seems to accommodate complicated local movements, due to dextral transtension in the Simplon area and compression in the Valais. The southern branch of the Pennine front is now accommodating local thrusting (less than 0.3 mm a^{-1}), decreasing toward the south to reach a locked state near the Argentera massif. The Periadriatic line is almost inactive, except along its western segment, where dextral slip rates reach 0.15 mm a^{-1}.

Models with rotational boundaries

Rotation may have played an important role in the dynamics of the western/central Alps, since at least Oligo-Miocene times (Gidon 1974; Anderson & Jackson 1987; Ménard 1988; Vialon *et al.* 1989; Thomas *et al.* 1999; Collombet *et al.* 2002). On the strength of GPS monitoring, involving French, Swiss and Italian stations (Calais *et al.* 2002), it is claimed that the Apulian promontory is rotating anticlockwise with respect to stable Europe at a rate of 0.52°/Ma, around a pole located at 45.36°N/9.10°S (near Milan).

In order to test the effects of such a rotation on the strain and stress field of the western/central Alpine arc, boundary nodes for the Po plain have been given appropriate velocities in model C (same three-dimensional crustal structure as model A) and model D (same three-dimensional crustal structure as model B).

In terms of stress (Figs 6 and 7), results for the rotation models appear to be quite similar to those for fixed models at a large scale. Orogen-perpendicular extensional stress is present in the internal zones, and orogen-perpendicular fan-like compression in the external zones (at least in the northwestern part). Only the regional/local pattern of stress axes is different from that of the fixed models. Thus rotation induces frontal compression at the eastern edge of the SW Alps and near the Po plain. This is especially true for model C, where compressional axes follow the rotational motion of boundary nodes. For model D, stress axes deviate less than for model C. This may be because GPAs are more variable in

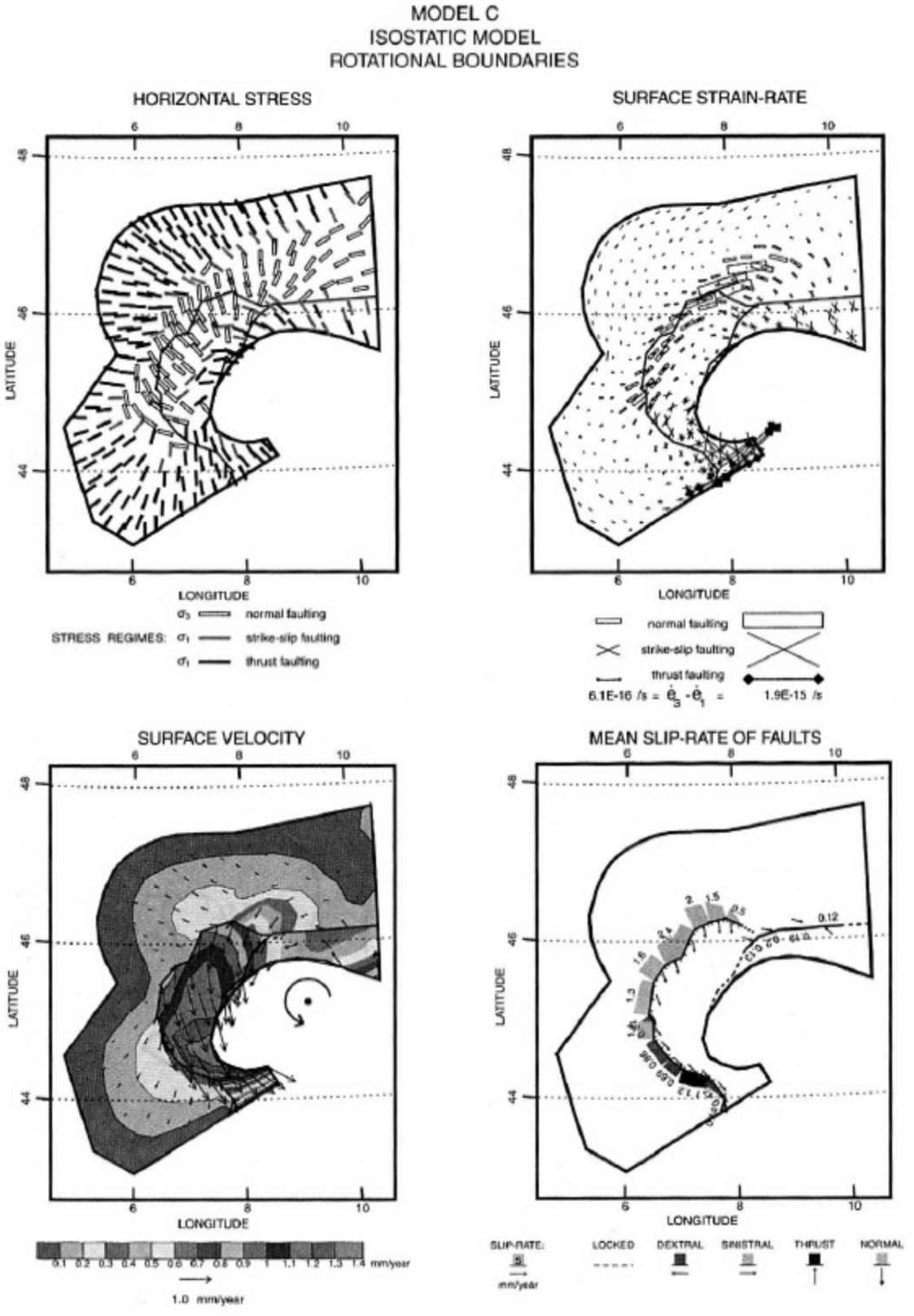

Fig. 6. Model C: Model with isostatic three-dimensional crustal geometry and rotational Po plain boundary nodes. See Figure 4 for comparison. Differences between models A and C are only due to rotational Po plain boundary. Curved arrow on surface velocity map indicates rotation pole (see text for explanation).

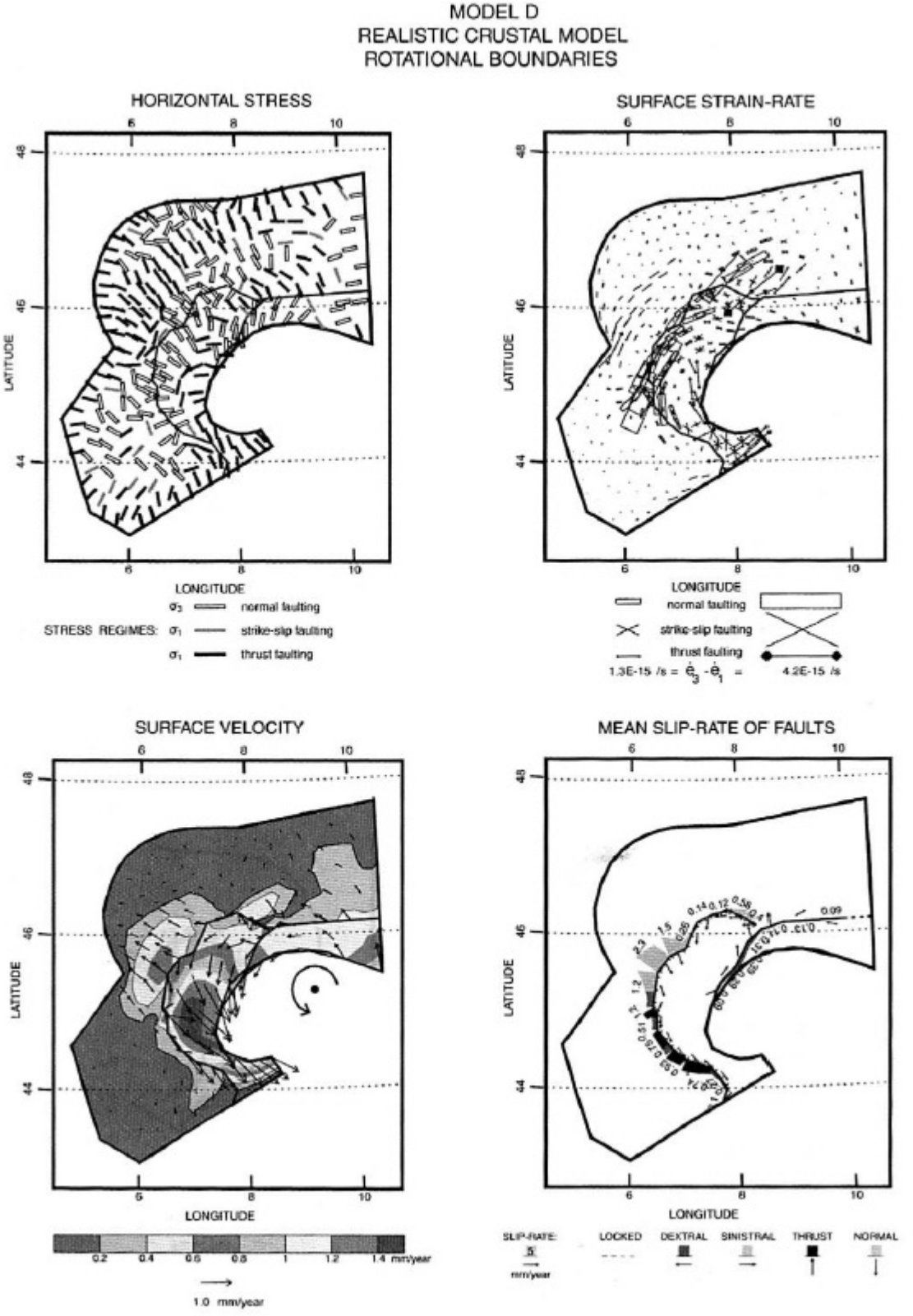

Fig. 7. Model D: Model with realistic three-dimensional crustal geometry and rotational Po plain boundary nodes. See Figure 5 for comparisons. Differences between models B and D are only due to rotational Po plain boundary (see text for explanation).

the non-isostatic model (model D), so that body forces are more dominant.

In terms of strain rate, as well as stress, axes are almost the same as for fixed models and only small regional reorientations are observed. The main differences are at boundaries. For example, at the south Ligurian boundary, anticlockwise rotation induces large shortening. Surface velocities of up to 1.4–1.5 mm a^{-1} concentrate in internal zones and appear to be strongly linked to the rotational boundary. Velocity vectors follow this rotation, pointing more to the south than for fixed models. Rotation seems to have little effect on velocities of external zones.

Slip directions along faults are more south-directed than those of fixed models. For the Pennine front, this implies S-verging stretching of up to 1.7 mm a^{-1} in the northern segment (model C), dextral transtension in the middle segment (1.1 $\pm$ 2 mm a^{-1} for model C, 2.1 mm a^{-1} for model D), and dextral transpression in the southern segment (1.4 mm a^{-1} for model C, 1.2 mm a^{-1} for model D). Another major difference with fixed models is the small dextral motion on the Periadriatic line (up to 0.22 mm a^{-1} for model C and 0.4 mm a^{-1} for model D).

Geodynamic implications

Numerical modelling and comparison with large-scale seismotectonic analysis have shown that body forces play a major role in determining the current stress field of the western Alpine arc. Balance of GPAs explains the orogen-perpendicular contrasted stress field in the western/central Alps (extensional in the core of the belt, locally compressional at the periphery). The role of rotational boundary forces is less obvious, as only local stress reorientations appear in our models. Nevertheless, rotation models seem suitable to explain dextral strike–slip faulting along the external zones (from the northern Valais to the Argentera massif). In addition, our results are consistent with GPS studies (e.g. Calais *et al.* 2002) that give velocities of about 1 mm a^{-1} within the Alpine realm, compatible with velocities of 1–1.5 mm a^{-1} obtained in the models of this study. More precisely, GPS studies reveal extension in the core of the belt, including lengthening of the line Lyon–Turin (0.5 $\pm$ 0.9 mm a^{-1} to the SE at La Feclaz in the Subalpine chains and 1.4 $\pm$ 0.4 mm a^{-1} to the SE at Modane (in the internal Vanoise area). This geodetic stretching correlates well with the values obtained for the core of the belt by seismotectonic analysis and numerical modelling. Moreover, GPS results also indicate shortening in the western Po plain (1.0–0.5 mm a^{-1} of E–W shortening between Modane and Turin) and in Provence (1.4–0.5 mm a^{-1} of N–S shortening between Grasse and Turin). Despite this qualitative agreement with the results of our modelling and seismotectonic analysis, more detailed comparisons cannot be made, because the GPS data still have insufficient resolution.

This study addresses the consequences of ongoing convergence between Europe and Africa. The convergence velocity is estimated at 3 $\pm$ 8 mm a^{-1} in a N to NW direction at the longitude of the Alps (Argus *et al.* 1989; Demets *et al.* 1990; Demets *et al.* 1994; Albarello *et al.* 1995; Crétaux *et al.* 1998; Kreemer & Holt 2001; Nocquet 2002). It could be taken up in different areas between the European and African stable continents, such as Northern Africa, the Apennines, the Dinarides or the Calabrian subduction zone. In the vicinity of the western/central Alpine arc, the interaction between boundary forces and body forces is still a matter for debate. Studies, such as the one by Thatcher *et al.* (1999) in the Basin and Range province, show that gravitational extensional tectonics can interact with boundary conditions, leading to reorientation of extensional axes parallel to plate tectonic directions. However, in our study, direct effects of plate tectonics are less useful to explain the stress field of the western/central Alps, which appears to be controlled mostly by internal body forces. A more detailed analysis of the possible interactions between boundary forces and body forces in the Alpine belt would require a detailed three-dimensional geometry of the models (accounting for lithospheric complexities), a fully three-dimensional finite element code, as well as more constraints on boundary conditions between Apulian and European microplates. Recent tomographic studies (Lippitsch 2002) have yielded a complex three-dimensional geometry at great depth, which has been interpreted in terms of lithospheric slabs, possibly detached in the western Alps and subvertical under the central Alps. These lithospheric structures cannot be modelled by the techniques used in this study. Their consequences for the current stress field and recent tectonics of the Alpine arc remain to be analysed.

Conclusions

A seismotectonic investigation along the entire arc of the western/central Alps has revealed contrasting stress regimes. Within a zone of extension that follows the arcuate crest line

from the southern Valais to the Argentera massif, extensional axes are perpendicular to the orogen. Compression is limited to the external zones, where compressional axes are also perpendicular to the orogen. Strike–slip faulting occurs in both external and internal zones, but is particularly abundant in the latter, where it is right-lateral, all the way from the northern Valais to the Durance fault (northwest of the Argentera massif). This well-defined seismotectonic stress state, comparable to the ones computed with 2.5D numerical modelling, highlights the essential role of gravitational body forces, which are able to produce orogen-perpendicular extension in the topographic highs and resulting orogen-perpendicular compression at the periphery. The role of rotation, which has been tested in our models, is more ambiguous, but could explain the arcuate right-lateral faulting prevailing in the external zones.

In a context of ongoing far-field convergence between the European and African plates, no direct evidence of collision has been found in the Alpine realm, either by seismotectonic analyses, numerical modelling, or GPS studies. This suggests that the current stress field in the western/central Alps is post-collisional.

Neuchâtel University and the Swiss National Science Foundation (grant # 21-61684.00) supported this study. We wish to thank Peter Bird for free online access to his finite element codes (http://element.ess.ucla.edu/); Jean Chéry and Rob Butler for their reviews; Peter Cobbold for his great help to the manuscript; and Nicole Béthoux, Jean-Mathieu Nocquet and Riad Hassani for fruitful discussions.

References

AHORNER, Z., MURAWSKI, H. & SCHEINDER, G. 1972. Sismotektonische Traverse von der Nordsee bis zum Apennin. *Geologische Rundschau*, **61**, 915–942.

ALBARELLO, D., MANTOVANI, E., BABBUCCI, D. & TAMBURELLI, C. 1995. Africa-Eurasia kinematics – main constraints and uncertainties. *Tectonophysics*, **243** (1–2), 25–36.

ANDERSON, H. & JACKSON, J. 1987. Active tectonics in the Adriatic region. *Geophysical Journal of the Royal Astronomical Society*, **91**, 937–983.

ARGUS, D. F., GORDON, R. G., DEMETS, C. & STEIN, S. 1989. Closure of the Africa-Eurasia-north America plate motion circuit and tectonics of the Gloria fault. *Journal of Geophysical Research*, **94**, 5585–5602.

BADA, G., HORVATH, F., CLOETINGH, S., COBLENTZ, D. & TOTH, T. 2001. Role of topography-induced gravitational stresses in basin inversion: the case study of the Pannonian basin. *Tectonics*, **20** (3), 343–363.

BAROUX, E., BÉTHOUX, N. & BELLIER, O. 2001. Analyses of the stress field in southeastern France from earthquake focal mechanisms. *Geophysical Journal International*, **145**, 336–348.

BECKER, A. 2000. The Jura Mountains – an active foreland fold-and-thrust belt? *Tectonophysics*, **321** (4), 381–406.

BIRD, P. 1989. New finite element techniques for modeling deformation histories of continents with stratified temperature-dependent rheology. *Journal of Geophysical Research*, **94** (B4), 3967–3990.

BIRD, P. 1999. Thin-plate and thin-shell finite-element programs for forward dynamic modeling of plate deformation and faulting. *Computers & Geosciences*, **25**, 383–394.

BIRD, P. 2002. Stress-direction history of the western United States and Mexico since 85 Ma. *Tectonics*, **21** (3), 5–12.

BISTACCHI, A., DAL PIAZ, G. V., MASSIRONI, M., ZATTIN, M. & BALESTRIERI, M. L. 2001. The Aosta-Ranzola extensional fault system and Oligocene – Present evolution of the Austroalpine-Penninic wedge in the northwestern Alps. *International Journal of Earth Sciences*, **90** (3), 654–667.

BISTACCHI, A., EVA, E., MASSIRONI, M. & SOLARINO, S. 2000. Miocene to Present kinematics of the NW-Alps: evidences from remote sensing, structural analysis, seismotectonics and thermochronology. *Journal of Geodynamics*, **30**, 205–228.

BLUNDELL, D., FREEMAN, R. & MUELLER, S. 1992. *A Continent Revealed: The European Geotraverse*. Cambridge University Press. Oxford, London, Edinburgh, Boston, Melbourne.

BURG, J. P., SOKOUTIS, D. & BONINI, M. 2002. Model-inspired interpretation of seismic structures in the Central Alps: Crustal wedging and buckling at mature stage of collision. *Geology*, **30**, 643–646.

BURKHARD, M. 1990. Aspects of the large-scale Miocene deformation in the most external part of the Swiss Alps (Subalpine Molasse to Jura fold belt). *Eclogae Geologicae Helvetiae*, **83** (3), 559–583.

BURKHARD, M. & SOMMARUGA, A. 1998. Evolution of the western Swiss Molasse basin: structural relations with the Alps and the Jura belt. *In*: MASCLES, A., PUIGDEFÀBREGAS, C., LUTERBACHER, H. P. & FERNÀNDEZ, M. (eds) *Cenozoic Foreland Basins of Western Europe*. Geological Society of London, Special Publications, **134**, 279–298.

BUTLER, R. W. H. 1992. Thrusting patterns in the NW French Subalpine chains. *Annales Tectonicae*, **6**, 150–172.

CALAIS, E., NOCQUET, J. M., JOUANNE, F. & TARDY, M. 2002. Current strain regime in the Western Alps from continuous Global Positioning System measurements, 1996–2001. *Geology*, **30**, 651–654.

CATTIN, R. & AVOUAC, J. P. 2000. Modeling mountain building and the seismic cycle in the Himalaya

of Nepal. *Journal of Geophysical Research*, **105** (B6), 13 389–13 407.

CATTIN, R., MARTELET, G., HENRY, P., AVOUAC, J. P., DIAMENT, M. & SHAKYA, T. R. 2001. Gravity anomalies, crustal structure and thermo-mechanical support of the Himalayas of Central Nepal. *Geophysical Journal International*, **147**, 381–392.

CHAMPAGNAC, J. D., SUE, C., DELACOU, B. & BURKHARD, M. 2003. Brittle orogen-parallel extension in the internal zones of the Swiss Alps (south Valais). *Eclogae Geologicae Helvetiae*, **96**, 325–338.

CHAMPAGNAC, J. D., SUE, C., DELACOU, B. & BURKHARD, M. 2004. Brittle deformation in the inner northwestern Alps: from early orogen-parallel extrusion to late orogen-perpendicular collapse. *Terra Nova*, **16**(4), 232–242, doi: 10.1111/j. 1365-31 21.2004.00555.x.

CHOUKROUNE, P., BALLÈVRE, M., COBBOLD, P., GAUTIER, Y., MERLE, O. & VUICHARD, J. P. 1986. Deformation and motion in the western alpine arc. *Tectonics*, **5** (2), 215–226.

COLLOMBET, M., THOMAS, J. C., CHAUVIN, A., TRICART, P., BOUILLIN, J. P. & GRATIER, J. P. 2002. Counterclockwise rotation of the western Alps since the Oligocene: new insights from paleomagnetic data. *Tectonics*, **21**, 352–366.

COWARD, M. & DIETRICH, D. 1989. Alpine tectonics: an overview. *In*: COWARD, M., DIETRICH, D. & PARK, R. (eds) *Alpine Tectonics*. Geological Society, London, Special Publications, **45**, 1–29.

CRÉTAUX, J.-F., SOUDARIN, L., CAZENAVE, A. & BOUILLÉ F. 1998. Present-day tectonic plate motions and crustal deformations from the DORIS space system. *Journal of Geophysical Research*, **103**, 30167–30181.

DAVIES, J. H. & VON BLANCKENBURG, F. 1995. Slab breakoff: A model of lithosphere detachment and its test in the magmatism and deformation of collisional orogens. *Earth and Planetary Sciences Letters*, **129** (1–4), 85–102.

DELACOU, B., SUE, C., CHAMPAGNAC, J. D. & BURKHARD, M. 2004. Present-day geodynamics in the bend of the western and central Alps as constrained by earthquake analysis. *Geophysical Journal International*, doi:10.1111/j.1365-1246X. 2004.02320.x.

DEMETS, C., GORDON, R. G., ARGUS, D. F. & STEIN, S. 1990. Current plate motions. *Geophysical Journal International*, **101**, 425–478.

DEMETS, C., GORDON, R. G., ARGUS, D. F. & STEIN, S. 1994. Effect of recent revisions to the geomagnetic reversal time scale on estimates of current plate motions. *Geophysical Research Letters*, **21**, 2191–2194.

DEWEY, J. F., HELMAN, M. L., TURCO, E., HUTTON, D. W. H. & KNOTT, S. D. 1989. Kinematics of the western Mediterranean. *In*: COWARD, M., DIETRICH, D. & PARK, R. (eds) *Alpine Tectonics*. Geological Society, London, Special Publications, **45**, 265–283.

DUCHÊNE, S., BLICHERT-TOFT, J., LUAIS, B., TÉLOUK, P., LARDEAUX, J. M. & ALBARÉDE, F. 1997. The Lu–Hf dating of garnets and the ages of the Alpine high-pressure metamorphism. *Nature*, **387**, 586–589.

EVA, E., PASTORE, S. & DEICHMANN, N. 1998. Evidence for ongoing extensional deformation in the Western Swiss Alps and thrust-faulting in the southwestern Alpine foreland. *Journal of Geodynamics*, **26** (1), 27–43.

EVA, E. & SOLARINO, S. 1998. Variations of stress directions in the western Alpine arc. *Geophysical Journal International*, **135**, 438–448.

FRÉCHET, J. 1978. *Sismicité du sud-est de la France et une nouvelle méthode de zonage sismique*. Thèse de doctorat d'Etat, Université des Sciences Technologiques et Medicales, Grenoble.

FRISCH, W., DUNKL, I. & KUHLEMANN, J. 2000. Post-collisional orogen-parallel large-scale extension in the Eastern Alps. *Tectonophysics*, **327** (3–4), 239–265.

FRY, M. 1989. Southwestward thrusting and tectonics of the Western Alps. *In*: COWARD, M., DIETRICH, D. & PARK, R. (eds) *Alpine Tectonics*. Geological Society, London, Special Publications, **45**, 83–109.

FÜGENSCHUH, B., LOPRIENO, A., CERIANI, S. & SCHMID, S. 1999. Structural analysis of the Subbriançonnais and Valais units in the area of Moûtiers (Savoy, Western Alps): paleogeographic and tectonic consequences. *International Journal of Earth Sciences*, **88**, 201–218.

GIDON, M. 1974. L'arc alpin a-t-il une origine tourbillonnaire? *Comptes Rendus de l'Académie des Sciences de Paris*, **278**, 21–24.

GOLKE, M. & COBLENTZ, D. 1996. Origins of the European regional stress field. *Tectonophysics*, **266** (1–4), 11–24.

GRÜNTHAL, G. & STROMEYER, D. 1992. The recent crustal stress field in Central Europe: trajectories and finite element modeling. *Journal of Geophysical Research*, **97** (B8), 11 805–11 820.

HASSANI, R. & CHÉRY, J. 1996. Anelasticity explains topography associated with Basin and Range normal faulting. *Geology*, **24** (12), 1095–1098.

KASTRUP, U. 2002. *Seismotectonics and stress-field variations in Switzerland*. PhD thesis, ETHZ, Zürich.

KONG, X. & BIRD, P. 1995. SHELLS: A thin-shell program for modeling neotectonics of regional or global lithosphere with faults. *Journal of Geophysical Research*, **100** (B11), 22 129–22 131.

KREEMER, C. & HOLT, W. E. 2001. A no-net-rotation model of present day surface motion. *Geophysical Research Letters*, **28**, 4407–4410.

LAUBSCHER, H. 1991. The arc of the Western Alps today. *Eclogae Geologicae Helvetiae*, **84** (3), 631–659.

LESNE, O., CALAIS, E. & DEVERCHERE, J. 1998. Finite element modeling of crustal deformation in the Baikal rift zone: new insights into the active-passive rifting debate. *Tectonophysics*, **289**, 327–340.

LIPPITSCH, R. 2002. *Lithosphere and upper mantle P-wave velocity structure beneath the Alps by high-resolution teleseismic tomography*. PhD thesis, ETHZ, Zurich.

LIU, Z. & BIRD, P. 2002. Finite element modeling of neotectonics in New Zealand. *Journal of Geophysical Research*, **107** (B12), 2328–2346.

MANCKTELOW, N. S. 1992. Neogene lateral extension during convergence in the Central Alps: evidence interrelated faulting and backfolding around the Simplonpass (Switzerland). *Tectonophysics*, **215**, 295–317.

MASSON, F., VERDUN, J., BAYER, R. & DEBEGLIA, N. 1999. Une nouvelle carte gravimétrique des Alpes occidentales et ses conséquences structurales et tectoniques. *Comptes Rendus de l'Académie des Sciences de Paris*, **329**, 865–871.

MAURER, H., BURKHARD, M., DEICHMANN, N. & GREEN, G. 1997. Active tectonism in the central Alps: Contrasting stress regimes north and south of the Rhone Valley. *Terra Nova*, **9**, 91–94.

MÉNARD, G. 1988. *Structure et cinématique d'une chaîne de collision: Les Alpes occidentales et centrales*. Thèse de Doctorat d'état, Université Joseph Fourier, Grenoble.

NEGREDO, A. M., BIRD, P., SANZ DE GALDEANO, C. & BUFORN, E. 2002. Neotectonic modeling of the Ibero-Maghrebian region. *Journal of Geophysical Research*, **107** (B11), 2292.

NOCQUET, J.-M. 2002. *Mesure de la déformation crustale en Europe occidentale par Géodésie spatiale*. Thèse de doctorat, Université de Nice.

NOCQUET, J. M. & CALAIS, E. 2003. Crustal velocity field of western Europe from permanent GPS array solutions, 1996–2001. *Geophysical Journal International*, **154** (1), 72–88.

NOCQUET, J. M. & CALAIS, E. 2004. Geodetic measurements of crustal deformation in the Western Mediterranean and Europe. *Pure & Applied Geophysics*, **161** (3), 661–681.

PAVONI, N. 1961. Faltung durch horizontal verschiebung. *Eclogae Geologicae Helvetiae*, **54**, 515–534.

PAVONI, N. 1986. Regularities in the pattern of major fault zones of the earth and the origin of arcs. *In*: WEZEL, F. C. (ed) *Origin of Arcs*. Elsevier, Amsterdam, 63–78.

POGNANTE, U. 1991. Petrological constraints on the eclogite- and blueschist-facies metamorphism and P-T-t paths in the Western Alps. *Journal of Metamorphic Geology*, **9**, 5–17.

RATSCHBACHER, L., FRISCH, W., LINZER, H.-G. & MERLE, O. 1991. Lateral extrusion in the Eastern Alps; part 2: structural analysis. *Tectonics*, **10** (2), 257–271.

SACHSENHOFER, R. F., KOGLER, A., POLESNY, H., STRAUSS, P. & WAGREICH, M. 2000. The Neogene Fohnsdorf Basin: basin formation and basin inversion during lateral extrusion in the Eastern Alps (Austria). *International Journal of Earth Sciences*, **89** (2), 415–430.

SCHMID, S. M. & KISSLING, E. 2000. The arc of the western Alps in the light of geophysical data on deep crustal structure. *Tectonics*, **19** (1), 62–85.

SPALLA, M. I., LARDEAUX, J. M., DAL PIAZ, G. V., GOSSO, G. & MESSIGA, B. 1996. Tectonic significance of Alpine Eclogites. *Journal of Geodynamics*, **21**, 257–285.

STAMPFLI, G. M., MOSAR, J., MARQUER, D., MARCHANT, R., BAUDIN, T. & BOREL, G. 1998. Subduction and obduction processes in the Swiss Alps. *Tectonophysics*, **296** (1–2), 159–204.

SUE, C. 1998. *Dynamique actuelle et récente des Alpes occidentales internes – Approche structurale et sismologique*. Thèse de doctorat, Université Joseph Fouriere, Grenoble.

SUE, C., THOUVENOT, F., FRÉCHET, J. & TRICART, P. 1999. Widespread extension in the core of the western Alps revealed by earthquake analysis. *Journal of Geophysical Research*, **104** (B11), 25 611–25 622.

SUE, C. & TRICART, P. 2002. Widespread Post-Nappe Normal Faulting in the Internal Western Alps: A New Constraint on Arc Dynamic. *Journal of the Geological Society*, **159**, 61–70.

SUE, C. & TRICART, P. 2003. Neogene to current normal faulting in the inner western Alps: a major evolution of the late alpine tectonics. *Tectonics*, **22** (5).

THATCHER, W., FOULGER, G. R., JULIAN, B. R., SVARC, J., QUILTY, E. & BAWDEN, G. W. 1999. Present-day deformation across the Basin and Range Province, Western United States. *Science*, **283**, 1714–1718.

THOMAS, J. C., CLAUDEL, M. E., COLLOMBET, M., TRICART, P., CHAUVIN, A. & DUMONT, T. 1999. First paleomagnetic data from the sedimentary cover of the French Penninic Alps: evidence for Tertiary counterclockwise rotations in the Western Alps. *Earth and Planetary Sciences Letters*, **171** (4), 561–574.

THOUVENOT, F. 1996. Aspects *géophysiques et structuraux des Alpes occidentales et de trois autres orogénèses (Atlas, Pyrénées, Oural)*. Thèse de doctorat d'Etat, Université Joseph Fourier, Grenoble.

TRICART, P., SCHWARTZ, S., SUE, C., POUPEAU, G. & LARDEAUX, J.-M. 2001. La dénudation tectonique de la zone ultradauphinoise et l'inversion du front briançonnais au sud-est du Pelvoux (Alpes Occidentales): une dynamique miocène à actuelle. *Bulletin de la Société Géologique de France*, **172** (1), 49–58.

VIALON, P., ROCHETTE, P. & MÉNARD, G. 1989. Indentation and rotation in the Alpine arc. *In*: COWARD, M., DIETRICH, D. & PARK, R. (eds) *Alpine Tectonics*. Geological Society, London, Special Publications, **45**, 329–338.

VIGNY, C., CHERY, J. *ET AL.* 2002. GPS network monitors the Western Alps' deformation over a five-year period: 1993–1998. *Journal of Geodesy*, **76** (2), 63–76.

WALDHAUSER, F., KISSLING, E., ANSORGE, J. & MUELLER, S. 1998. Three-dimensional interface modelling with two-dimensional seimic data: the Alpine crust–mantle boundary. *Geophysical Journal International*, **135**, 264–278.